

Optical Reflectivity Spectrum of a CuFeS₂ Single Crystal

Tamio OGUCHI,* Katsuaki SATO and Teruo TERANISHI

Broadcasting Science Research Laboratories of Nippon Hoso Kyokai, Tokyo 157

(Received June 27, 1979)

Optical reflectivity spectra have been measured at room temperature on a single crystal of CuFeS₂ between 0.025 and 6 eV. The experimental results have been used to calculate the optical constants, the dielectric constant and the absorption coefficient. There have been found an absorption band with peaks at 1.0 and 2.1 eV and an absorption edge at approximately 3.2 eV. The band can be assigned to the charge-transfer transition from the valence band to the empty 3d states of Fe, and the edge can be attributed to the commencement of the band to band transition. A schematical energy level diagram for CuFeS₂ is given from the result.

§1. Introduction

The optical absorption edge of an antiferromagnetic semiconductor CuFeS₂ has been known to exist at approximately 0.5 eV.¹⁾ This value is anomalously small compared with that of other chalcopyrite type semiconductors such as CuAlS₂ (3.4 eV)²⁾ and CuGaS₂ (2.5 eV).³⁾

Based on absorption measurements of CuAlS₂: Fe and CuGaS₂: Fe and on molecular orbital calculations, we came to the conclusion that the absorption edge of CuFeS₂ is not the "band to band" edge in usual sense but is the foot of the "charge-transfer" absorption band associated with 3d-orbitals of Fe ions.^{4,5)} Absorption measurements on thin polycrystalline films of CuFeS₂ revealed that CuFeS₂ has a broad absorption band at 0.6–3.5 eV region similar to that of CuAlS₂: Fe and CuGaS₂: Fe as predicted by the previous work.⁶⁾

The purpose of the present work is to get more accurate informations on the electronic structure of CuFeS₂ by means of the reflectivity measurement between 0.025 and 6 eV on single crystals of CuFeS₂.

The remainder of the paper consists of four sections; experimental techniques in §2, experimental results in §3, discussions in §4 and conclusions in §5.

§2. Experimental Techniques

Large single crystals of CuFeS₂ about 10

mm in diameter and a few cm in length were grown from melt by the Bridgman method. Specimens for measurements were cut from the boule into disk with thickness of approximately 2 mm and were polished mechanically by using alumina grinding powder, followed by sheets of lapping film (3M Inc.) of several grain size (9 μm, 3 μm, 1 μm, 0.3 μm). Polished samples were then rinsed in the ultrasonic water bath to get rid of the grinding powder.

The obtained surface showed a mirror-like golden luster which is characteristic of the chalcopyrite. The crystal orientation of the polished surface was determined by the X-ray Laue photography to be very close to (112) crystal plane.

Reflection measurements were performed using a Nikon P-250 monochromator with a specially designed double beam reflectance attachment as illustrated in Fig. 1. The principle of the measurement is as follows:—Light is split into two beams by BS; one is led to the sample, and the other to a reference mirror; two beams are chopped at different frequencies, by small-size rotating sectors (C₁, C₂); reflected beams are focused together onto the window of a light detector (D). The sample-channel signal (I_S) and the reference-channel signal (I_R) are separately amplified by lock-in amplifiers tuned to each frequency, and the ratio I_S/I_R is then taken by means of the feedback technique. The output data were punched on paper tape and processed by an off-line computer for further analysis; —correction of reflectivity of the reference mirror, data smoothing, Kramers-Kronig analysis.

* On leave from The University of Electro-Communications, Chofu, Tokyo 182.

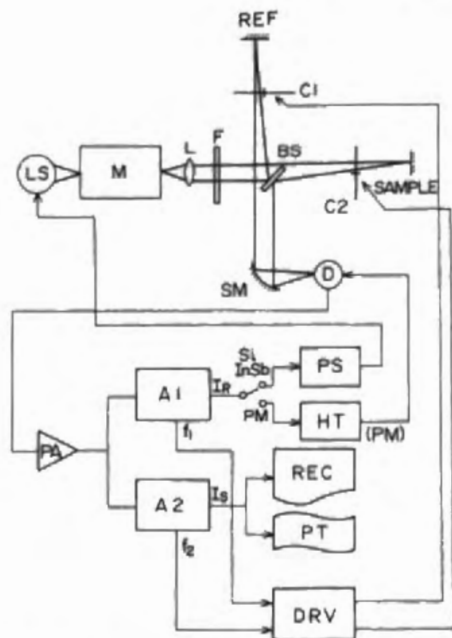


Fig. 1. A schematic diagram of the apparatus for reflectivity measurement. LS: Light Source (deuteron or halogen-tungsten lamp), M: Monochromator (Nikon P-250; gratings with blaze wavelengths of 350, 750 and 2000 nm), L: Fused Silica lens, F: Glass-filters against higher order light, BS: Beam splitter (double faced mirror), C1 and C2: Light-chopper with rotating sector, SM: Spherical mirror, D: Light detector (Photomultiplier, Silicon photocell, or cooled InSb-photocell), PA: Preamplifier, A1, A2: Lock-in amplifiers, PS: Power supply for LS, HT: High-voltage supply for photomultiplier, REC: Chart recorder, PT: Perforated paper tape, DRV: Chopper driver.

Since the measurement covers fairly wide wavelength region (near u.v. to near i.r.), total region was divided into several sections and a suitable combination of optical elements were selected for every section, as listed in Table I.

To get i.r. data ($2.5 \mu\text{m}$ to $50 \mu\text{m}$) we employed a Hitachi 255 infrared spectrophotometer with a reflectance attachment (IRR-3).

Optical constants n and k measured at 632.8 nm by means of the ellipsometry have been used to calibrate the calculated values.

All measurements were performed at room temperature.

§3. Experimental Results

Optical reflectivity spectrum of the single crystal surface of CuFeS_2 between 0.025 and 6 eV measured at room temperature is shown in Fig. 2. The curve is a composition of reflectivity spectra for several spectral regions mentioned in the previous section.

The spectrum is characterized by a steep rise of R (reflectivity) below 0.2 eV , two peaks at 1 to 2 eV region and a strong dip around 3.2 eV . The yellowish color of this material is due to the strong dip of R at "blue" wavelength region.

Optical constants n and k were calculated by using the Kramers-Kronig relations,⁷⁾ with appropriate extrapolations for wavelengths beyond the region of measurement. Values of parameters for the analysis were so determined that calculated values of n and k at 632.8 nm

Table I. Combinations of optical elements used in our measurement for the eight wavelength regions listed in the first column.

Region (nm)	Light source	Grating		Mirror coating	Detector	Filter
		Blaze (nm)	Grooves (G/mm)			
200- 400	D	300	600	Al	PM	—
250- 600	H-T	300	600	Al	PM	UV-35
400- 800	H-T	300	600	Ag	Si	UV-35/Y-50
550-1000	H-T	750	600	Ag	Si	Y-50
700-1300	H-T	750	600	Ag	Si	R-67
1000-1600	H-T	750	600	Ag	InSb	IRD-80A
1300-2000	H-T	2000	300	Ag	InSb	IRD-80A
1800-2600	H-T	2000	300	Ag	InSb	IRD-80A+G-54

D: Deutron lamp, H-T: Halogen-tungsten lamp, PM: Photo-multiplier (Hamamatsu R636), Si: Silicon-photocell (Hamamatsu S-875-66R), InSb: Cooled InSb-photocell (Hamamatsu P839S), Filters: (Toshiba glass filters), UV-35 (350 nm cut-off), Y-50 (500 nm cut-off), R-67 (670 nm cut-off), IRD-80A (900-4500 nm band-pass), G-54 (1000-4500 nm band-pass).

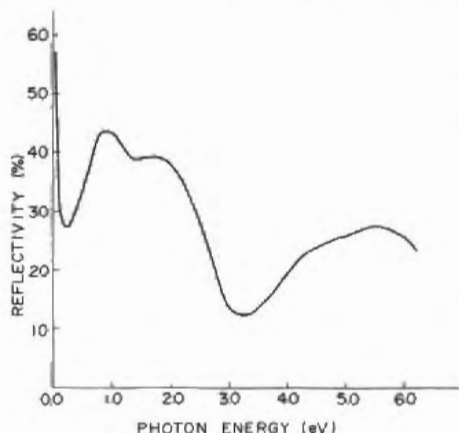


Fig. 2. The reflectivity spectrum of CuFeS₂ measured at room temperature.

fit those calibrated by means of the ellipsometry. In Fig. 3, spectra of n and k thus obtained are illustrated by a solid curve and a dotted curve, respectively.*

Optical absorption coefficient α was calculated from the k by the formula,

$$\alpha = \frac{4\pi k}{\lambda},$$

where λ is the wavelength. The absorption spectrum thus obtained is given in Fig. 4.

* Strictly speaking, optical constants n and k should be expressed in tensor form for CuFeS₂, which belongs to the tetragonal crystal system. However, since the tetragonality is rather small, we treat them, for simplicity, as scalar quantities in the present paper.

The curve consists of a broad band between 0.6 and 3.2 eV and an absorption edge rising from approximately 3.2 eV. The broad band can be decomposed into two Gaussian components with centers at 1 eV (peak A) and 2.1 eV (peak B) as plotted by dotted curves in the same figure. By subtracting these two Gaussian curves from the original absorption spectrum the higher energy absorption edge (C) has been distinguished as shown by dashed curve.

Real and imaginary parts of the dielectric constant $\epsilon = \epsilon' + i\epsilon''$ was also calculated from n and k and are shown in Fig. 5 together with the dielectric loss function $Im(-1/\epsilon)$. It should be noted that ϵ' is negative for photon energies below 0.07 eV and for 2.0 to 2.5 eV.

In Fig. 6 is given a curve of n_{eff} , effective number of electrons per CuFeS₂ unit contributing to the optical transitions below the photon energy of consideration. The n_{eff} has been calculated by the following formula,

$$n_{eff}(\omega) = \frac{m}{2\pi^2 Ne^2} \int_0^\infty \omega' \epsilon''(\omega') d\omega',$$

where N is a number of CuFeS₂ molecules per cm³, m is the free electron mass and ϵ'' is the imaginary part of dielectric constant. It is noted that for usual semiconductors such as Si, n_{eff} saturates at a value of approximately 4 per atom; on the other hand for CuFeS₂, n_{eff} shows a plateau at nearly 0.25 electron per atom (~one electron per CuFeS₂) below 3 eV and rises again at higher energies, showing no

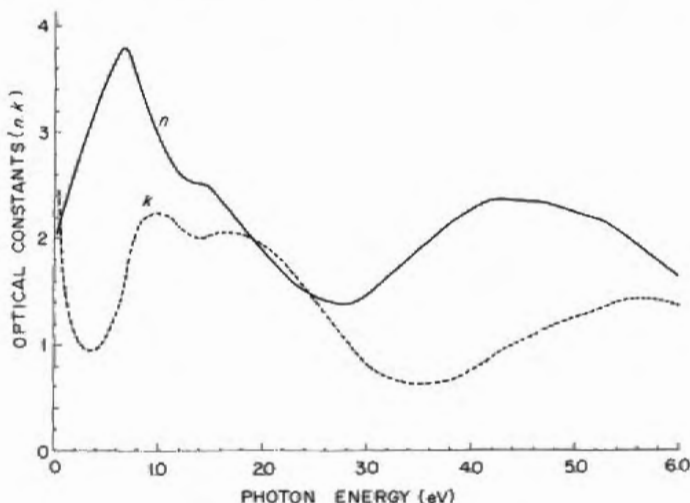


Fig. 3. The optical constants, n (solid curve) and k (dotted curve) of CuFeS₂ as calculated from the reflectivity spectrum.

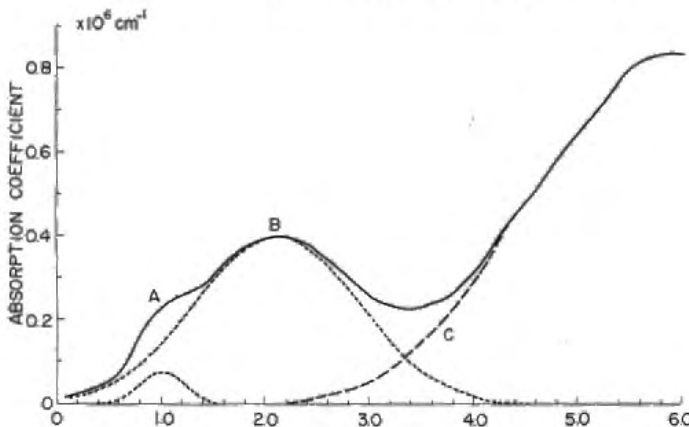


Fig. 4. The absorption spectrum of CuFeS_2 as calculated from k by using the formula $\alpha = 2k\omega/c$ (solid curve). Two Gaussian curves (dotted curves) are fitted to reproduce peaks A and B. Dashed curve represents the absorption edge C.

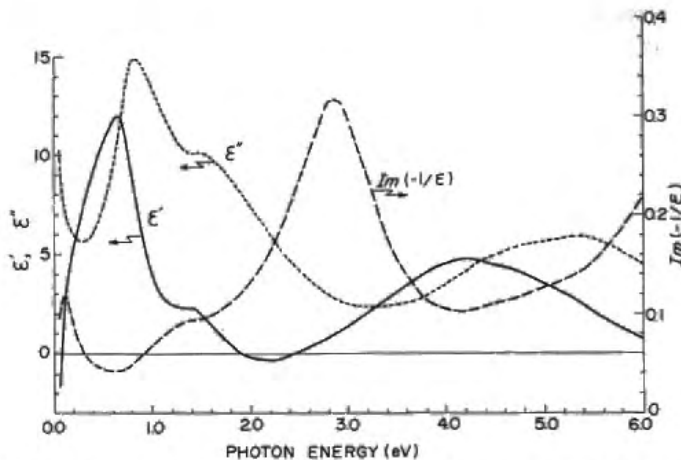


Fig. 5. The spectral dependence of the dielectric constant $\epsilon = \epsilon' + i\epsilon''$ (left scale) and the dielectric loss function (right scale); solid curve— ϵ' , dotted curve— ϵ'' , dashed curve—loss function, $\text{Im}(-1/\epsilon)$.

saturation up to 6 eV.

§4. Discussions

In the first place, the absorption spectrum (Fig. 4) obtained by the present study is compared with that directly measured on polycrystalline film reported in ref. 6: Although the energy positions of two peaks A and B in two curves are very similar, the value of absorption coefficient of the present study is smaller by a factor of about 3 than the previous value for film. This difference may possibly be brought about from the ambiguity in evaluating the film thickness.

Secondly, the absorption curve is compared with that of CuAlS_2 : Fe reported in ref. 4. We can find similar absorption peaks A and B

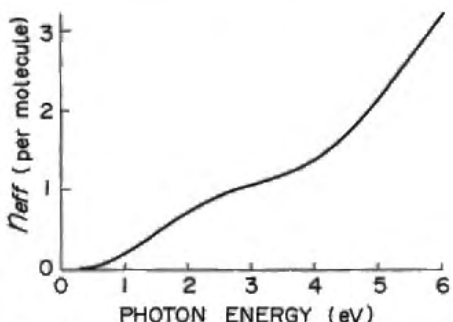


Fig. 6. The curve of n_{eff} , effective number of free electrons contributing to the optical constant up to the frequency of consideration.

in both curves; energy positions, half-widths and oscillator strengths of peaks A and B are listed in Table II for CuFeS_2 and $\text{CuAl}_{0.99}$

Table II. Energy positions (E), half-widths (ΔE), and oscillator strengths (f) of peaks A and B for CuFeS₂ (present study) and CuAl_{0.99}Fe_{0.01}S₂ (ref. 4).

	Peak-A			Peak-B		
	E (eV)	ΔE (eV)	f	E (eV)	ΔE (eV)	f
CuFeS ₂	1.0	0.5	7×10^{-3}	2.1	1.86	3.5×10^{-1}
CuAl _{0.99} Fe _{0.01} S ₂	1.3	0.25	5×10^{-3}	1.9	0.8	0.9×10^{-1}

Fe_{0.01}S₂. The table shows that energy positions and oscillator strengths are very close between two cases, although the band widths of CuFeS₂ is about twice those of CuAl_{0.99}Fe_{0.01}S₂. Therefore it is natural to assume that absorption peaks A and B of CuFeS₂ have the same origin as those of CuAl_{0.99}Fe_{0.01}S₂;—the charge transfer from valence band to d-orbitals of Fe.

It has been known from previous works that although 3d states in CuAl_{1-x}Fe_xS₂ are sufficiently localized to be described in terms of the multiplet 6A_1 , when x is much less than 0.1,⁹ they are rather extended to form "3d-bands" due to hybridization with p-orbitals of anions when x exceeds 0.1.^{10,11} This is consistent with the present result that band widths of peak A and B of CuFeS₂ is twice those of CuAl_{0.99}Fe_{0.01}S₂.

In the third place, it is seen in Fig. 3 that k increases steeply as the photon energy decreases below 0.4 eV. This increase is attributed to so-called Drude-tail which is caused by the plasma oscillation of the free electron gas. The plasma frequency v_p can be estimated by the energy where ϵ' crosses zero from negative to positive in Fig. 5; $hv_p = 0.07$ eV. It is well known that the charge concentration can be estimated by the formula,

$$N = \frac{v_p^2 \pi m}{e^2}$$

where m is the free electron mass and e is the electronic charge. By applying $hv_p = 0.07$ eV we obtain

$$N = 3.46 \times 10^{18} \text{ cm}^{-3},$$

which is a reasonable value for synthetic CuFeS₂.

Next we discuss the curve of n_{eff} shown in Fig. 6. As stated in §3 n_{eff} does not saturate at a value of 4 per atom as seen in Si but has a plateau with a value of 0.25 per atom (1.0 per CuFeS₂ molecule) below 3 eV. Therefore the

absorption band below 3 eV cannot be assigned to the usual "band to band" transition as seen in Si but can be assigned to a transition transferring one electron per molecule from the valence band to the empty "3d" band. A change of slope of n_{eff} curve which occurs around 3.2 eV may be interpreted as the beginning of the "band to band" transition of this material.

Finally, based on the experimental results of the present study and on the theoretical calculations by Kambara a schematic energy-level diagram for CuFeS₂ has been constructed and is shown in Fig. 7.

The composition of the atomic orbitals consisting each energy level determined by the theoretical study is also added in the figure.

The empty "3d"-band is located between valence and conduction band. The observed optical band gap of 0.5 eV corresponds to the

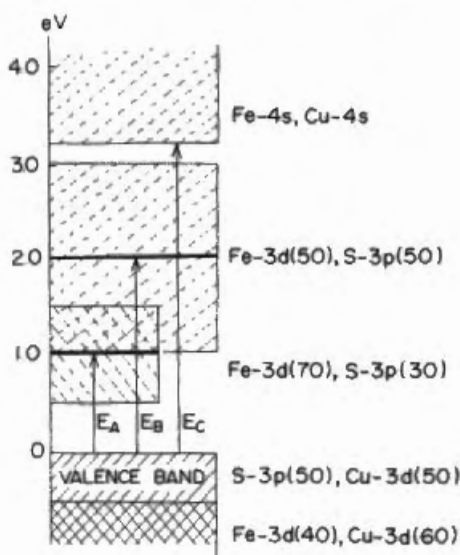


Fig. 7. A schematic energy-level diagram based on the optical properties of CuFeS₂. The leading constituent atomic orbitals and their composition ratio for each level obtained from the theoretical study⁴ are also given in the right hand column.

energy separation between the "3d" band and the valence band. E_A , E_B are the energies associated with the maxima of the joint density of states between these bands. The bandwidth of the "3d" band cannot be unambiguously determined, since observed bandwidth is related to both "3d" and valence bands; so that the value shown in Fig. 7 may be regarded as the upper limit of the 3d bandwidth. The fact that photoconduction has been observed in the vicinity of the optical band gap indicates that the 3d band forms a conducting state.

The bottom of the 4s-conduction band is determined as 3.2 eV above the top of the valence band from the energy position where n_{eff} curve changes its slope. The theoretical calculation has given rather wrong values for the energy separation between valence and 4s-band; 6 eV. The discrepancy may possibly be caused by the crudeness of the theoretical calculation. The molecular orbital calculation for the atomic cluster cannot account for precise features of the extended states as it lacks considerations of the periodic boundary conditions.

Although the temperature of our study have been restricted to room temperature, we believe that most of the arguments discussed above on the electronic structures of CuFeS₂ is still valid for low temperature state: A preliminary measurement at liquid nitrogen temperature showed no marked shift nor measurable splitting of the spectra at least for visible wavelength region.

It is a future problem to examine the fine structure by means of low temperature studies or any kind of modulation spectroscopies, which would be effective for further understanding of the electronic structures of this material.

§5. Conclusions

In the present work the reflectivity spectrum measurements have been performed and the optical constants and the schematical energy-level diagram for CuFeS₂ have been deduced from the results. The absorption spectrum

calculated from the optical constant essentially agrees with that measured directly for the thin polycrystalline film.

The position of the empty "3d" band has been determined by this work to locate in the gap between the valence and the 4s-conduction bands. The bandwidth of the "3d" band of CuFeS₂ has been found to be approximately twice that of CuAl_{0.99}Fe_{0.01}S₂ where 3d states are thought to be localized.

Since it has been known from our previous work¹¹⁾ that a jump of R occurs when Fe-content in CuAl_{1-x}Fe_xS₂ is increased across the critical value of $x \sim 0.1$, at which content the resistivity and the effective magnetic moment show an abrupt change, it is desirable to measure reflectivity spectrum precisely for CuAl_{1-x}Fe_xS₂ samples with various content of iron in the vicinity of $x \sim 0.1$.

Acknowledgements

The authors are very grateful to Professor K. I. Gondaira and Professor T. Kambara for valuable discussions. They are also indebted to Mr. Kiichi Kobayashi of the NHK Technical Laboratories for his help on the ellipsometric measurement.

References

- 1) C. H. L. Goodman and R. W. Douglas: Physica **20** (1954) 1107.
- 2) W. N. Honeyman: J. Phys. Chem. Solids **30** (1969) 1935.
- 3) B. Tell, J. L. Shay and H. M. Kasper: Phys. Rev. **B4** (1971) 2463.
- 4) T. Teranishi, K. Sato and K. Kondo: J. Phys. Soc. Jpn. **36** (1974) 1618.
- 5) T. Kambara: J. Phys. Soc. Jpn. **36** (1974) 1625.
- 6) K. Sato and T. Teranishi: J. Phys. Soc. Jpn. **40** (1976) 297.
- 7) F. Stern: Solid State Phys. **15** (1963) 327.
- 8) H. R. Philipp and H. Ehrenreich: Phys. Rev. **129** (1963) 1550.
- 9) K. Sato and T. Teranishi: J. Phys. Soc. Jpn. **37** (1974) 415.
- 10) T. Teranishi and K. Sato: J. Phys. (France) **36** (1975) C3, 149.
- 11) T. Teranishi and K. Sato: *Ternary Compounds* (1977) (Inst. Phys. Conf. Ser. No. 35) p. 59.